REGRESSION RELATIONSHIPS BETWEEN SATELLITE INFRARED RADIANCE AND TROPOSPHERIC TEMPERATURE

Bruce William Hepner

NAVAL POSTGRADUATE SCHOOL
Monterey, California

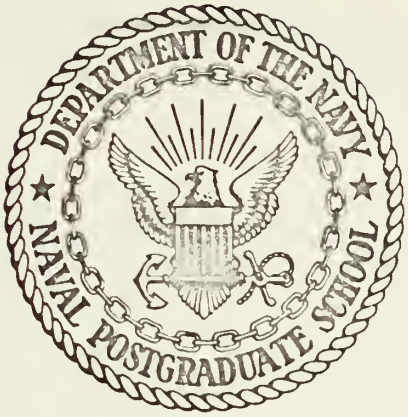

THESIS

Regression Relationships Between Satellite Infrared Radiance and Tropospheric Temperature

by

Bruce William Hepner

Thesis Advisor: F. L. Martin

March 1972

Regression Relationships Between Satellite Infrared Radiance and Tropospheric Temperature

by

Bruce William Hepner
Lieutenant, United States Navy
B.S., Purdue University, 1964

Submitted in partial fulfillment of the
requirements for the degree of

MASTER OF SCIENCE IN METEOROLOGY

from the

NAVAL POSTGRADUATE SCHOOL
March 1972

ABSTRACT

Global temperatures are obtained using a linear least squares regression method with satellite radiation measurements, particularly those obtained from the SIRS-B aboard the NIMBUS IV satellite. Regression equations relating temperature to spectral radiance observations are employed. The regression equations were then applied to independent observations to determine the feasibility of temperature determinations over sparse data regions.

TABLE OF CONTENTS

LIST OF TABLES

TABLE OF SYMBOLS AND ABBREVIATIONS

A	Product of cloud-cover and cloud-emissivity
ADP	Automatic data processing
$B(\nu_i,T)$	Planck intensity function at wavenumber ν_i and temperature T
C_i	Regression coefficients of the ith variable added
CO_2	Carbon dioxide
F_k	F-ratio upon entry at step k
FNWC	Fleet Numerical Weather Central
GMT	Greenwich Mean Time
i	Channel number
IBM	International Business Machines
K	Degrees Kelvin
mb	Millibars
$N(\nu_i)$	Spectral radiance observed at wavenumber ν_i
N_c	Corrected radiance
NESC	National Environmental Satellite Center
NMC	National Meteorological Center
p	Atmospheric pressure
p_c	Atmospheric pressure at cloud-top
p_s	Atmospheric pressure at earth surface
S.E.	Standard error
T	Temperature (^oK)
T_F	Interpolated FNWC temperature
T_N	NESC-generated temperature

Table of Symbols and Abbreviations (continued)

$T(p)$	Vertical distribution of temperature as a function of pressure
σ	Standard deviation
τ	Fractional transmittance

ACKNOWLEDGEMENTS

The author wishes to express his appreciation to his advisor, Professor F. L. Martin, for his suggestions, advice, guidance and support in this research.

Appreciation is also expressed to the author's wife and family for their patience and understanding during the period of work on this thesis.

Appreciation is also expressed to the W. R. Church Computer Center Facility of the Naval Postgraduate School.

I. INTRODUCTION

The launch of the NIMBUS IV on 8 April 1970 was the second step in a process of developing a means of determining the three-dimensional state of the atmosphere by indirect means. The orbit of the NIMBUS IV was a near-circular, polar-orbit, with a height of approximately 600 nm. The new instrument, known as SIRS-B (which is similar to the instrument on NIMBUS III, known as SIRS-A)) has the added capabilities of "side looking" scan for greater area coverage, and the determination of the tropospheric water vapor content.

The calibration procedure used to transform the radiation sensed in the eight channels of the SIRS-B to spectral radiances is discussed in the NIMBUS IV USERS GUIDE (1970). The temperature profile of the atmosphere within the field of view, comprising an area of $(225km)^2$ at the subsatellite point, is deduced using the channel spectral-radiance ensemble. The particular wavenumbers sensed are small intervals in the atmospheric window and the 15-micron band of CO_2. The channel numbers and wavenumbers are listed:

$CH._i$ NO.	1	2	3	4	5	6	7	8
WAVE. NO. $\nu_i (cm^{-1})$	899.0	750.0	734.0	709.0	701.0	692.0	679.8	668.7

Through the equation of radiative transfer, the measured radiances are related to the temperature-structure T(p) of the atmosphere, the temperature at the earth's surface and that at the cloud tops which may be within the field-of-view. Assuming that a single cloud layer exists, the following set of integral equations can be constructed for the measured radiance $N(\nu_i)$ in channel i:

$$N(\nu_i)=A\left\{ B[\nu_i,T(p_c)]\tau(\nu_i,p_c) - \int_1^{\tau_c} B[\nu_i,T(p)]d\tau(\nu_i,p) \right\}$$
$$+ (1-A)\left\{ B[\nu_i T(p_s)]\ \tau(\nu_i,p_s) - \int_1^{\tau_s} B[\nu_i,T(p)]d\tau(\nu_i,p) \right\} \quad (1)$$

i=1, 2, . . . , 8 is the channel number.

$N(\nu_i)$ = spectral radiance at wavenumber ν_i.

$B[\nu_i,T(p)]$ = Planck radiance at wavenumber ν_i and temperature, (Eq. (3) below).

$\tau(\nu_i,p)$= fractional transmittance of the atmosphere in the spectral interval centered at wavenumber ν_i and assumed known as a function of the pressure p at the radiating level.

A = the product of the fraction of cloud cover within the field-of-view and the cloud emissivity (which is usually assumed to be unity).

Subscripts c and s refer to cloud-top and earth surface.

The special case of equation (1) where A=0 gives the clear-column or corrected radiance $N_c(\nu_i)$. This term is contained within the second brace of equation (1). It is this quantity which must be determined in all channels in

order to convert the corrected radiance set into a vertical temperature profile T(p). The clear-column spectral radiance at the top of the atmosphere at wavenumber ν_i is therefore:

$$N_c(\nu_i) = B[\nu_i, T(p_s)]\tau(\nu_i, p_s) - \int_1^{\tau_s} B[\nu_i, T(p)]\, d\tau(\nu_i, p_s) \qquad (2)$$

where

$$B[\nu_i, T(p)] = c_1 \nu_i^3 \left\{ \exp\left[c_2 \nu_i / T(p)\right] - 1 \right\}^{-1} \qquad (3)$$

is the Planck function at wavenumber ν_i.

Here T=T(p) is the temperature (assumed to be in thermodynamic equilibrium at level p), and c_1 and c_2 are known constants

$$c_1 = 1.9061 \times 10^{-5} \text{ erg cm}^2 \text{ sec}^{-1} \text{ ster}^{-1}$$

$$c_2 = 1.43868 \text{ cm } ^{o}\text{K}$$

$\tau(\nu_i, p)$ is the transmittance at wavenumber ν_i of the atmosphere above level p.

Smith, Woolf and Jacobs (1970) have used equations (2) and (3) to <u>define</u> a weighted-mean black-body temperature $T_{B,i}$ in terms of the corrected radiance $N_c(\nu_i)$ which would be observed from an atmosphere of structure T=T(p)

$$N_c(\nu_i) = B(\nu_i, T_{Bi}) \qquad (4)$$

Here T_{Bi} is independent of pressure. Solving the relationships (3) and (4) for T_{Bi} gives

$$T_B(\nu_i) = c_2 \nu_i / \ln\left\{ \left[c_1 \nu_i^3 / N_c(\nu_i)\right] + 1 \right\} \qquad (5)$$

Smith et al (1970) have provided multiple regression equations which relate NMC effective grid point temperature

$T(p_j)$ at SIRS-A scan spots to the sixteen predictors $T_B(\nu_i)$ and $T_B(\nu_i)^2$. They have done this by relating a two-week NMC data file of temperatures at standard pressure levels p_j to the corrected radiances, and arrived at an equation of the form

$$T(p_j) = T(p_j) + \sum_{i=1}^{8} a(\nu_i, p_j)[T_B(\nu_i) - \bar{T}_B(\nu_i)] + \sum_{i=1}^{8} a'(\nu_i, p_j)\,[T_B(\nu_i) - \bar{T}_B(\nu_i)]^2 \qquad (6)$$

A similar study will be made for T(500) and T(300) using a data-base of corrected radiances from SIRS-B and NESC derived temperature profiles $T(p_j)$ together with simultaneous FNWC effective grid-point soundings (available from the Fleet Numerical Weather Central ADP tapes) at locations of the scan-spots in both space and time. For the SIRS-B data file, a revised NESC formula similar to equation (6) was available for the conversion of corrected radiance-sets into a statistically consistent profile T=T(p).

II. DATA PROCESSING

A. THE ORIGINAL DATA

The original data utilized in this paper were provided by the National Environmental Satellite Center (NESC), and consisted of computer listings of a selected set of SIRS-B scan spots recorded during December 1970. In addition to the geographical coordinates and time of each observation, there were also listed the raw (uncorrected) radiances in each channel. The raw radiances are assumed to be derived from equation (1) for the one cloud-layer model and the corrected radiances resulted from the systematic elimination of cloud contamination effects from each channel [following a technique of Smith et al (1970)].

The atmospheric window channel (channel 1) was inoperative during this period; therefore, the values of the corrected window channel were chosen from locations where the surface temperature, based on the NMC data file, was known to be at a pressure-level close to $p \doteq 1000$ mb, where T_s is known. Furthermore, since the radiance-correction computation involves iterative use of equations (2) and (6)(using an equivalent "clear-column" temperature profile, $T=T(p)$, at each iteration), all original radiance-sets chosen could thus be "tied down" by the selection of scan-spots having surface pressure values $p_s = 1000$ mb, with T_s known.

It should be noted that the data samples provided were enhanced by the side-viewing capability of the SIRS-B. The side-viewing capability enabled the scanning of more atmosphere-earth columns both on and off the subtrack for which the approximation p_s = 1000 mb was valid. Slant-columns thus viewed are useful for reduction to clear-column temperature profiles T = T(p) after the slant path is normalized to a single atmospheric depth over the spot viewed.

In general, virtually all scan spots have some effective cloud cover (A > 0) in view of the large area $(225\ km)^2$ being viewed. Of the seven CO_2 channels being used, the two channels subject to the maximum attenuation by the interposition of a "cool" cloud top within the desired T = T(p) profile are channels 2 and 3.

Smith, Woolf, and Jacobs (1970) have indicated the procedure involved for correcting for cloud-contamination of the eight channels of radiances. Based upon the actual NMC climatological update of each of the standard pressure-levels, (10, 30, 50, 100, 150, 200, 250, 300, 400, 500, 700, 850, and 1000 mb) they have derived multiple regression equations relating $T(p_j)$ to the clear-column-radiance $N_c(\nu_i)$, or to the blackbody temperature-equivalent of the clear-column radiance. For example, Smith et al (1970) obtained regression equations essentially of the form of equation (6) and have listed the least-squares best-fit coefficients obtained for a period in September 1969 applicable in a zonal band 35-55°N. As a second approximation,

Smith et al have also generated a six-predictor analog of equation (6) with channels 2 and 3 deleted for the same time frame as utilized for the eight-predictor equation. In both cases, they have deduced equation (6) and its six-predictor analog by employing a large sample-size of simultaneous values of corrected radiance-sets and of values of $T(p_j)$ (at standard pressure levels), interpolated from the NMC file to the location of the SIRS scan spot. The six-predictor and eight-predictor regression equations are continually updated to a revised two-week data base after three additional data-days are accumulated. Such equations were also available during the SIRS-B period of December 1970.

The procedure for correction of the ith channel radiance makes iterative use of the updated SIRS-B operational six-predictor regression equation in deducing a first guess of $T=T(p)$. At the first guess, the uppermost five radiances $(N_4,\ldots,N_8)$ which are least affected by cloud contamination are used as the first guess correct-radiance set, together with the prescribed N_1 from the window-channel blackbody "fix" at the scan spot. With these six-predictors known, a first guess of the temperature profile, $T(p_j)$, at all standard levels is computed. After the first-guess of the temperature profile is made, the profile is then applied to channels 2 and 3 to determine the "best fit" for cloud height and effective cloud cover A using equation (1), rewritten for simplicity as

$$N(\nu_i) = (1-A)\, N_c[\nu_i, T(p), p_s] + AY\,[\nu_i, T(p), p] \qquad (7)$$

Here Y represents the contents of the first brace of equation (1). Also $c(\nu_i)$ is defined as

$$c(\nu_i) = N_c\,(\nu_i) - N(\nu_i) \qquad (8)$$

for the correction to be applied to the radiances for channels 4 through 8. Writing equation (7) for channels 2 and 3 in terms of the corrected values of N_c based on T(p) (the clear-column temperature) and the corresponding computation of Y from the top of the clouds gives two simultaneous equations. From these two simultaneous equations, one solves for the two unknowns, A and p_c, using indirect methods for solving for p_c (i.e. making separate tests for p_c = 200, 250, ..., 850 mb) and, in turn, determining the value of A which "best-fits" equation (7) expressed in terms of $N(\nu_2)$ and $N(\nu_3)$. These values of A and p_c are substituted into equation (7) for a second corrected estimate of $N_4,\ldots,N_8$ and a new temperature profile is calculated. The iterative procedure is continued in this manner and usually converges within four iterations, i.e., the correction $c(\nu_i)$ of (8) usually converges

$$c(\nu_i) \rightarrow c(\nu_i, \text{ limit})$$

for a suitable tolerance within four iterations. At this point, the finalized temperature profile T(p) may be used to compute the clear-column radiances for channels 2 and 3 as well as the five uppermost CO_2 channels using Eq. (1). Cloud influence is thus compensated when the final choice of temperature profile has been made.

In a sizeable fraction of the cases selected, the convergence $c(\nu_i)$ required more than four iterations which means that a relaxed requirement for convergence had to be employed. This generally occurred with cloud tops at or above 500 mb. Such cases of below-normal attenuation recovery were indicated on the NESC data-listings as decreased reliability. Nevertheless, no data cases were discarded for such reasons.

B. ADJOINING OF FNWC DATA

Analyzed temperature-field data for 500 and 300 mb covering the period from 00 GMT 24 December 1970 through 00 GMT 29 December 1970 was provided by Fleet Numerical Weather Central (FNWC). The FNWC temperature data had not been correlated with radiances as was the NESC data. The FNWC temperature fields at 500 and 300 mb [$T_F(5)$ and $T_F(3)$] were spatially and temporally interpolated to obtain consistency with the SIRS soundings. Spatial interpolation was accomplished using Bessel's central-difference interpolation [Haltiner, 1971] to the latitude and longitude of the SIRS-B soundings. Temporal interpolation to the time of the scan-spot was accomplished utilizing linear interpolation between temperature fields preceding and succeeding the time of the SIRS sounding. These methods were employed to obtain statistical dependence of $T_F(5)$ and $T_F(3)$ upon the corrected radiance set $N_1,\ldots,N_8$. This necessitated the printout of

FNWC interpolated temperatures in a format consistent with the requirements of the program BIMED 02R, to be used in (III).

C. DATA DESIGNATION

The original NESC data comprised some 207 to 329 scan-spots per day and were identified by the specific time of the SIRS soundings and their latitude and longitude. The original FNWC data tapes consisted of temperatures at the levels 300 and 500 mb, at each grid point of the 63 x 63 Northern Hemisphere FNWC grid. The FNWC data at scan spots were obtained by interpolation as previously described.

A three-day data base of both NESC and FNWC data was then compiled using data from 0600 GMT to 1800 GMT for 24, 25, and 26 December 1970. A four-day data base was compiled by the addition of data from 0600 to 1800 GMT 27 December 1970 to the three-day data base. Data sets for independent regression tests were compiled using data centered on 00 and 12 GMT 27 December and 00 and 12 GMT, 28 December (i.e., data-base times plus 12 and 24 hours).

All data sets were divided into three bands. These bands were bounded by latitudes: 20-40°N, band 1; 35-55°N, band 2; and 50-70°N, band 3. The bands were overlapped to reduce the possibilities of discontinuities across the boundaries when regression calculations were made.

The designation of dependent and independent variables was made and the dependent variable was designated T(i,j) and the independent variables were designated as shown:

CH. NO.	1	2	3	4	5	6	7	8
WAVE NO.	899.0	750.0	734.0	709.0	701.0	692.0	679.8	668.7
VAR. NO.	N_1	N_2	N_3	N_4	N_5	N_6	N_7	N_8

For each scan spot selected in the test period, the time and location were encoded on IBM cards, as were the temperatures $T_N(5)$, $T_N(3)$, $T_F(5)$, $T_F(3)$. Here, the subscript N indicates an NESC-generated temperature, using the convergent procedure described previously, and the subscript F denotes interpolated FNWC temperatures. Also encoded onto IBM cards were the eight channels of corrected radiances(provided by NESC using the method described in II.A.) for each of the scan spots. All data were encoded in a manner consistent with the requirements of the stepwise regression program, BIMED 02R (Dixon 1966) which will be discussed later.

III. THE REGRESSION METHOD

A. THE STEPWISE REGRESSION PROCEDURE

Many problems in research require the extensive analysis of large amounts of data. The data handling process should be made as automatic and rapid as possible. The appropriate tools for analyzing large data samples with numerous independent variables often require multivariate statistical regression techniques to attack the problem. The Biomedical Computer Programs (Dixon 1966) were developed to provide the techniques necessary for the statistical and mathematical analyses required. One of these programs is the Stepwise Regression Analysis Program BIMED 02R.

BIMED 02R computes, in a stepwise manner, a sequence of multiple linear regression equations. One variable is added to the regression equation at each step. The variable added is that which accomplishes the greatest reduction in the previously unexplained sum of squares. This variable is also the one which has the highest partial correlation with the dependent variable at the particular step in the analysis of the variance. Equivalently it is the variable which would have the highest F-value if it were added. The F-value, or F-statistic upon entry, F_k is expressed at step k as (Dixon 1966)

$$F_k(1,n-k-1) = \frac{\%(C.E.V.k) - \%(C.E.k-1)}{\%(U.E.V.,k)}$$

where

%(C.E.V.k) is the percent cumulative explained variance, step k.

%(C.E.V.k-1) is the percent cumulative explained variance, step k-1.

%(U.E.V.k) is the percent unexplained variance remaining at step k.

This study utilized a statistical model expressible in the form

$$T = C_o+C_1N_1+C_2N_2+C_3N_3+C_4N_4+C_5N_5+C_6N_6+C_7N_7+C_8N_8 \quad (9)$$

where C_o through C_8 are to be determined by the stepwise least squares technique. Equation (9) may be expressed in the more compact form utilizing the matrix-product equation

$$T = (C_o, C_1, \ldots\ldots, C_8)\begin{pmatrix} 1 \\ N_1 \\ \vdots \\ N_8 \end{pmatrix} \quad (10)$$

In (10), the notation $T_N(3,5)$ will be used when the NESC data at 300 or 500 mb (respectively) are correlated against the predictors $(N_1,\ldots\ldots,N_8)$; whereas $T_F(3,5)$ is the notation for the corresponding predictands with FNWC temperatures. Equation (10) may also be used in application with independent data occurring up to 12 or 24 hours later than the dependent sample which yielded the particular coefficient matrix $(C_o, C_1 \ldots\ldots, C_8)$.

B. RELATED STATISTICAL PARAMETERS

Available as outputs from the BIMED 02R program are several related statistical parameters. Among these statistical parameters are:

a. multiple R

b. standard error of estimate, S. E.

c. mean value, $\bar{T}$

d. standard deviation σ

e. F-value

f. R^2

The significance of R^2 in relationship to S. E. is as follows (Crow et al 1955):

$$(S.E.)^2 = \sigma^2 \, [(n-1)/(n-k-1)] \, (1-R^2) \qquad (11)$$

where

$$\sigma^2 = \sum_{i=1}^{n} (T_i - \bar{T})^2/n$$

is the variance of the temperature sample, and

n = sample size

i = sample-element index

k = number of predictors

Furthermore, R is the multiple correlation coefficient after k predictors are added, with emphasis on k=8, in order to derive maximum information from the SIRS-sounding. It follows that the percentage unexplained variance $(1-R^2)$ for sample sizes in the range 171 to 228 as contained in the dependent data sample are very closely approximated by

$$(S.E./\sigma)^2 = 1-R^2$$

The percentage explained variance is then given by R^2; that is

$$R^2 = 1 - (S.E./\sigma)^2 \qquad (12)$$

since $(n-k-1)/(n-1)$ is close to unity for the dependent

sample sizes considered here. The factor (n-k-1)/(n-1) becomes (n-2)/(n-1) ≐ 1 for the independent test cases considered since in this case, there is only one way of forming the predictor to be listed.

C. THE REGRESSION PROCEDURE APPLIED TO THE DEPENDENT SAMPLES

The test on the dependent data was made using the least-squares, stepwise regression technique of BMD 02R to develop the coefficients $C_o, C_1, \ldots, C_8$. The coefficients for the three-day and four-day dependent samples for the T(5) and T(3) regression equations were computed by use of this technique. This test was performed on both the NESC-regression generated data and the interpolated FNWC data. The coefficients for the NESC three-day data sample are listed in Table 1, part (a) for 500 mb; and part (b) for 300 mb. Table 2 contains similar results for the four-day sample base of NESC data. The coefficients for the FNWC data are listed in Table 3 (three-day case) and Table 4(four-day).

The relevant statistics for the tests on the several dependent data bases are listed in Table 5 and 6. The statistics included in these tables are the mean, standard deviation, R^2, and standard error. A discussion of the statistics of prime interest is provided in IV.

TABLE 1. Regression coefficients for NESC dependent data.

(a) 500 mb, three-day sample

CONST	20-40N	35-55N	50-70N
C_0	-43.1058	-52.2372	-90.9234
C_1	-0.0327	0.4187	0.1508
C_2	-0.0932	-0.4795	-0.2562
C_3	0.8922	-0.2670	0.0
C_4	0.6949	3.0232	2.9128
C_5	-1.8871	-2.6461	-1.7719
C_6	-0.9188	-0.0726	-0.1134
C_7	0.4129	0.1608	0.2351
C_8	0.6664	0.0764	-0.1635

(b) 300 mb, three-day sample

C_0	-70.5523	-113.6468	-108.4219
C_1	0.4109	0.5032	0.3409
C_2	-0.2953	-0.3192	-0.2337
C_3	-1.4766	-1.4030	-0.6563
C_4	3.0286	3.1138	1.3928
C_5	-0.7404	0.0857	1.0938
C_6	-0.5295	0.0*	0.1261
C_7	-0.5835	-1.0623	-1.1938
C_8	0.6865	0.4809	0.3922

*indicates that this variable (*) was not accepted because it failed to explain appreciably

TABLE 2. Regression coefficients for NESC dependent data.

(a) 500 mb, four-day sample

CONST	20-40N	35-55N	50-70N
C_0	-48.6906	-51.8292	-92.4865
C_1	0.0	0.4842	0.1143
C_2	-0.0907	-0.6454	-0.1644
C_3	0.8032	-0.1472	-0.0980
C_4	0.6590	3.0011	3.0117
C_5	-1.5652	-2.6431	-1.7844
C_6	-0.9017	0.0*	-0.1327
C_7	0.2990	0.1605	0.1894
C_8	0.6797	0.0354	-0.1311

(b) 300 mb, four-day sample

C_0	-101.7840	-108.5859	-108.1667
C_1	0.1288	0.5599	0.3757
C_2	-0.0794	-0.5138	-0.3326
C_3	-0.2788	-1.0924	-0.5185
C_4	0.5219	2.7352	1.2617
C_5	1.2700	0.1432	1.1646
C_6	-1.0121	0.0*	0.1026
C_7	-0.5885	-1.0406	-1.2316
C_8	1.0295	0.5160	0.4386

*indicates that this variable (*) was not accepted because it failed to explain appreciably

TABLE 3. Regression coefficients for FNWC dependent data.

(a) 500 mb, three-day sample

CONST	20-40N	35-55N	50-70N
C_0	-15.6121	-55.3823	-85.1272
C_1	0.3605	0.4119	9.0638
C_2	-0.8342	-0.8714	-0.7219
C_3	0.7760	0.9170	1.7073
C_4	1.2602	1.6287	0.6259
C_5	-1.8509	-1.9698	-0.6344
C_6	-0.9308	0.1453	-0.1520
C_7	0.2310	-0.1858	0.0*
C_8	0.4440	0.1834	-0.0545

(b) 300 mb, three-day sample

C_0	-56.7715	-107.1405	-99.6836
C_1	0.4459	0.2963	0.3651
C_2	-0.6807	0.0459	-0.6303
C_3	-0.3890	-1.1144	0.3020
C_4	1.9185	2.1166	0.5930
C_5	-0.5798	0.3357	0.9944
C_6	-0.9211	-0.1590	0.0444
C_7	-0.2675	-0.5875	-0.6276
C_8	0.5916	0.2311	0.0392

*indicates that this variable (*) was not accepted because it failed to explain appreciably

TABLE 4. Regression coefficients for FNWC dependent data.

(a) 500 mb, four-day sample

CONST	20-40N	35-55N	50-70N
C_0	-15.3487	-51.3814	-88.3277
C_1	0.4477	0.5272	0.0260
C_2	-1.0928	-1.2317	-0.5774
C_3	1.0306	1.3415	1.4995
C_4	1.1163	1.3383	0.8176
C_5	-1.7344	-1.9340	-0.6736
C_6	-0.8981	0.2096	-0.1147
C_7	0.2645	-0.1328	-0.0979
C_8	0.3767	0.1141	0.0*

(b) 300 mb, four-day sample

C_0	-53.5409	-103.0841	-99.9952
C_1	0.4850	0.3744	0.3821
C_2	-0.7624	-0.1827	-0.6721
C_3	-0.4110	-0.8859	0.3722
C_4	2.0702	2.0795	0.5005
C_5	-0.6480	0.1929	1.0677
C_6	-0.8955	-0.1818	0.0171
C_7	-0.1607	-0.5045	-0.6575
C_8	0.4292	0.2066	0.0757

*indicates that this variable (*) was not accepted because it failed to explain appreciably

IV. DEPENDENT DATA RESULTS

The detailed results of the tests on dependent data are available in Tables 5 and 6. However, the essential portions needed for comparisons by the different tests using dependent data have been listed in Table 7 where the values of fractional explained variance as originally listed in Tables 5 and 6 are summarized. Also listed in Table 7 are the values of R^2 averaged over the data-base specification period (or mode) for each band as well as the values of R^2 averaged over the bands for a given data-base mode. Comparisons between regressions were based on the fractional explained variance R^2 rather than on the values of standard errors, as R^2 has been normalized with respect to the sample variances, which vary between bands.

The third value listed in the band columns of both parts (a) and (b) of Table 7 is the average over the data-base modes in each band. The values listed in the mode-average row and band-average column are the overall averages by the statistical regression. Comparisons of R^2 are made of the overall averages and of band averages, as well as data-base mode averages at both the 500-and 300-mb levels. Differences in values of certain compared R^2 are termed "% shrinkage" in the explained variance arising from the specification tests under comparison.

A. COMPARISON OF NESC SPECIFICATION STATISTICS

Examination was first made of the left hand side of Table 7 for comparison of the NESC regression results at 300 mb relative to those at 500 mb. The outstanding result of this comparison reveals $R_N^2(3)$ to be smaller than $R_N^2(5)$ by 0.1660, or 16.6% when averaged over bands 1, 2, and 3. Upon comparison of individual band results (averaged over the three and four day specification modes) one finds the same order of shrinkages distributed over the bands, namely, an average of 16.6%, but with a larger than normal shrinkage in band 2 where the value of R_N^2 fell off to 0.6857.

Upon use of the four-day estimation equation (10) in the respective cases (left side of Table 7) there was a small shrinkage in explained variance (relative to the three-day results) at both the 300- and 500-mb levels. This result was not quite anticipated since Smith et al found it advisable to use data-banks of two weeks for specification. Nevertheless, the small differences between the R_N^2 for the two prediction-base methods, whether at 300 or 500 mb, were not large enough to be considered significant in the tests conducted here.

B. COMPARISON OF FNWC SPECIFICATION STATISTICS

Here our comparisons will mainly concern the right hand side of Table 7. Again, predictor-mode differences seem to be marginal so that for the present they will be disregarded.

Comparison of $R_F^2(3)$ with $R_F^2(5)$ shows that band average shrinkage in the amount $R_F^2(5) - R_F^2(3) = 0.1480$ occurs. A breakdown of this statistic by bands shows shrinkage in the amounts 9.16%, 22.39%, and 12.87% for bands 1, 2, and 3, respectively.

Comparisons made between NESC and FNWC regression results (left side and right side of Table 7) show approximately 2% difference between $R_F^2(5) = 0.8737$ and $R_N^2(5) = 0.8957$ and less than 0.5% difference at the 300-mb level. Thus, the FNWC specifications at both levels explained very nearly as much variance as did the NESC results. There were some variations between bands, but generally, the same geographic pattern persisted throughout: namely, moderate to high R^2 in bands 1 and 3, with the lowest value in R^2 occurring in band 2. This was true of all FNWC specifications (300 and 500 mb) as well as of the NESC 300 mb specification. The NESC 500 mb specification gave rise to an increase in R^2 with an increase in latitude.

In summary, both NESC and FNWC regression equations tested well in terms of explained variance at 500 mb. Both showed diminished specification at 300 mb to values of $R^2 \doteq 0.73$. Finally, in no case was there a significant change when testing the four-day data base results against those for the three-day data base.

TABLE 5. Dependent-data temperature specification statistics resulting from pooled samples of NESC data.

Band	Sample Size	Mean	Std. Dev.	R^2	Std. Error
(a) 500 mb, three-day sample base					
20-40N	171	-15.5029	6.8730	0.8533	2.6970
35-55N	191	-28.3298	6.9763	0.9113	2.1218
50-70N	177	-34.1469	7.0397	0.9321	1.8724
(b) 500 mb, four-day sample base					
20-40N	206	-15.4369	6.7276	0.8379	2.2275
35-55N	228	-28.1623	6.7376	0.9040	2.1202
50-70N	216	-34.2176	7.0982	0.9358	1.8336
(c) 300 mb, three-day sample base					
20-40N	171	-42.7895	4.6668	0.7719	2.2834
35-55N	191	-50.4869	4.7427	0.6842	2.7152
50-70N	177	-54.6667	3.9610	0.7833	1.8874
(d) 300 mb, four-day sample base					
20-40N	206	-42.7233	4.6398	0.6548	2.7809
35-55N	228	-50.3509	4.6875	0.6871	2.6637
50-70N	216	-54.7778	3.9610	0.7970	1.8186

TABLE 6. Dependent-data temperature specification statistics resulting from pooled samples of FNWC data.

(a) 500 mb, three-day sample base

Band	Sample Size	Mean	Std. Dev.	R^2	Std. Error
20-40N	171	-15.9520	6.6156	0.8760	2.3861
35-55N	191	-28.2174	7.3512	0.8704	2.7045
50-70N	177	-34.2333	7.3384	0.8816	2.5767

(b) 500 mb, four-day sample base

20-40N	206	-15.9179	6.4674	0.8651	2.4232
35-55N	228	-28.0130	7.1574	0.8598	2.7283
50-70N	216	-34.2405	7.3470	0.8894	2.4842

(c) 300 mb, three-day sample base

20-40N	171	-42.2974	5.2983	0.7833	2.5267
35-55N	191	-50.8692	4.6688	0.6413	2.8571
50-70N	177	-54.9912	4.3548	0.7494	2.2313

(d) 300 mb, four-day sample base

20-40N	206	-42.3044	5.1558	0.7747	2.4962
35-55N	228	-50.7638	4.6363	0.6411	2.8276
50-70N	216	-55.1295	4.3142	0.7641	2.1354

TABLE 7. Summary of NESC and FNWC dependent regression test results.

	(a) NESC 500 mb				FNWC 500 mb			
	Band 1	Band 2	Band 3	Band Avg.	Band 1	Band 2	Band 3	Band Avg.
Three-day	0.8533	0.9113	0.9321	0.8989	0.8760	0.8704	0.8816	0.8760
Four-day	0.8379	0.9040	0.9358	0.8928	0.8651	0.8598	0.8894	0.8714
Period Avg.	0.8456	0.9076	0.9339	0.8957	0.8706	0.8651	0.8855	0.8737

	(b) NESC 300 mb				FNWC 300 mb			
	Band 1	Band 2	Band 3	Band Avg.	Band 1	Band 2	Band 3	Band Avg.
Three-day	0.7719	0.6843	0.7833	0.7465	0.7833	0.6413	0.7494	0.7247
Four-day	0.6548	0.6871	0.7970	0.7129	0.7747	0.6411	0.7641	0.7266
Period Avg.	0.7134	0.6857	0.7902	0.7297	0.7790	0.6412	0.7568	0.7257
	0.7795	0.7966	0.8620	0.8174	0.8248	0.7532	0.8212	0.7997

V. INDEPENDENT DATA TEST RESULTS

Verification of the dependent regression equations was accomplished using the regression coefficients (described in III) and the 12-and 24-hour independent data samples. The equations of form (10) developed from both the three-day and four-day samples were tested. The independent tests generate equations of the general form

$$T(5,3) = B_0 + B_1\tilde{T}(5,3) \qquad (13)$$

where B_0 and B_1 are regression constants and $\tilde{T}$ represents the temperature-estimators from the dependent regression equation (10) with coefficients appropriate to the level, the band and the mode-stratifications (Tables 1,2,3,4). The regression analysis for these tests is similar to the techniques applied in IV in that $\tilde{T}(5,3)$ is compared by regression methods to the observed temperature at each scan-spot. The results of the independent tests are given in Tables 8, 9, 10, and 11. Table 12 is constructed in a manner similar to that used to develop Table 7. The major difference between Tables 12 and 7 is that the 12- and 24-hour independent samples are statistically pooled in application of the independent regression test in order to obtain a larger sample size for each band, and also for ease of comparisons. The results of the pooled independent data verifications are presented in Table 12.

Internal comparisons of the values of fractional explained variance for the independent data yielded results quite similar to those obtained from the dependent data. The comparisons are stratified in two manners; by bands and by modes, as well as by levels.

A. COMPARISONS OF NESC INDEPENDENT VERIFICATIONS

From the left side of Table 12, it is easily observed that the largest overall average $R^2 = 0.8392$ occurred in connection with the 500-mb verification of $T_N(5)$. The corresponding mean NESC result at 300 mb verified with a percentage explained variance $R_N^2(3) = 0.7533$, i.e., with a shrinkage of 8.59% relative to $R_N^2(5)$.

As noted in IV(A and B), both NESC dependent specifications (300 and 500 mb) in band 3 verified highest with R^2 ranging between 0.82 and 0.91. The previously noted trend in R^2 continues at the 500-mb level of independent data with R^2 increasing poleward from 0.78 in band 1 to 0.91 in band 3. At 300 mb, this band distribution of $R_N^2(3)$ is not so apparent since values close to 0.72 are associated with bands 1 and 2 with a mean value of $R_N^2(3) \simeq 0.82$ existing in band 3.

B. COMPARISONS OF FNWC INDEPENDENT VERIFICATIONS

Comparisons of the FNWC independent tests (Table 12, right side) bring out primarily the same results which have been developed from dependent base samples. For example, the FNWC overall $R_F^2(5) \simeq 0.78$ may be compared with

$R_F^2(3) \simeq 0.75$. In general, the independent $R_F^2(3,indep)$ is close to the values found for $R_F^2(3,dep)$. In keeping with earlier results, band 2 has a relative minimum value of $R_F^2(indep)$ of magnitude 0.6760. The corresponding results for $R_F^2(5,indep)$ relative to $R_F^2(3,indep)$ show that the former averages, band-for-band, between 6 and 8% higher than the latter. Comparison of FNWC and NESC independent tests, both at 500 mb, shows higher mean specification of the latter by close to 5% in favor of NESC over FNWC independent verification in bands 2 and 3. The NESC verification stability seems to be dominant in bands 2 and 3 with values of $R^2 \simeq 0.85$. Here again, the geographic trend previously noted is present.

As has been described before, $R_F^2(5,indep)$ also has a band-2 minimum but at a level of 10% higher than $R_F^2(3,indep)$.

TABLE 8. Statistical results of the application of Eq. (10) to NESC independent-test samples at 500 mb.

(a) Three-day base estimator applied to independent sample

BAND	SAMPLE SIZE	OBSERVED MEAN	OBSERVED STD. DEV.	R^2	STD. ERROR	PROG TIME
20-40N	23	-15.8261	5.5239	0.8317	2.3195	12HR
	35	-15.1143	6.0477	0.7454	3.0973	24HR
35-55N	31	-29.1935	5.3130	0.7504	2.6995	12HR
	37	-27.2973	5.3534	0.8445	2.1724	24HR
50-70N	32	-34.7812	6.6027	0.9000	2.1229	12HR
	39	-34.5384	7.4440	0.9586	1.5356	24HR

(b) Four-day estimator applied to independent sample

20-40N	28	-15.1786	5.3958	0.7791	2.5841	12HR
	57	-14.5965	7.0530	0.8125	3.0821	24HR
35-55N	33	-26.9091	6.2917	0.8492	2.4823	12HR
	50	-28.2400	6.6350	0.8382	2.6967	24HR
50-70N	26	-34.1923	6.2802	0.8658	2.3482	12HR
	47	-33.7660	6.5846	0.9061	2.0396	24HR

TABLE 9. Statistical results of the application of Eq. (10) to NESC independent-test samples at 300 mb.

(a) Three-day base estimator applied to independent sample

BAND	SAMPLE SIZE	OBSERVED MEAN	OBSERVED STD. DEV.	R^2	STD. ERROR	PROG. TIME
20-40N	23	-41.1304	4.2672	0.8314	1.7933	12HR
	35	-42.3999	4.5581	0.7100	2.4915	24HR
35-55N	31	-51.9677	4.6725	0.7393	2.4267	12HR
	37	-49.6486	4.3857	0.6865	2.4905	24HR
50-70N	32	-56.3125	4.0595	0.8987	1.3362	12HR
	39	-55.2820	3.9732	0.8573	1.5421	24HR

(b) Four-day base estimator applied to independent sample

20-40N	28	-42.9643	4.3587	0.7532	2.2066	12HR
	57	-41.8246	4.0932	0.6648	2.3913	24HR
35-55N	33	-51.5151	3.8007	0.6823	2.1764	12HR
	50	-50.7000	4.8033	0.7310	2.5172	24HR
50-70N	26	-54.7308	4.2573	0.8712	1.5591	12HR
	47	-55.3191	4.0653	0.7123	2.2045	24HR

TABLE 10. Statistical results of the application of Eq. (10) to FNWC independent-test samples at 500 mb.

(a) Three-day estimator applied to independent sample

BAND	SAMPLE SIZE	OBSERVED MEAN	OBSERVED STD. DEV.	R^2	STD. ERROR	PROG. TIME
20-40N	23	-15.3869	5.2862	0.7992	2.4246	12HR
	35	-15.7514	5.7731	0.7922	2.6715	24HR
35-55N	31	-28.7902	6.4929	0.7463	3.3265	12HR
	37	-26.9594	6.0373	0.7617	2.9889	24HR
50-70N	32	-35.1687	6.8719	0.6570	4.0911	12HR
	39	-34.2743	7.4819	0.8674	2.7609	24HR

(b) Four-day estimator applied to independent sample

20-40N	28	-15.1714	4.8327	0.8056	2.1711	12HR
	57	-14.9736	6.3392	0.8032	2.8376	24HR
35-55N	33	-26.4999	6.6488	0.7611	3.3017	12HR
	50	-28.3659	7.0272	0.7536	3.5244	24HR
50-70N	26	-34.1691	7.1998	0.7257	3.8488	12HR
	47	-34.2914	7.0092	0.8486	2.7573	24HR

TABLE 11. Statistical results of the application of Eq. (10) to FNWC independent-test samples at 300 mb.

(a) Three-day base estimator applied to independent sample

BAND	SAMPLE SIZE	OBSERVED MEAN	OBSERVED STD. DEV.	R^2	STD. ERROR	PROG. TIME
20-40N	23	-41.1130	4.1381	0.8220	1.7868	12HR
	35	-42.3390	4.4627	0.6997	2.4823	24HR
35-55N	31	-52.4193	5.4097	0.6712	3.1551	12HR
	37	-50.2215	4.4871	0.6099	2.8425	24HR
50-70N	32	-57.0562	4.7833	0.8554	1.8490	12HR
	39	-55.7589	4.1201	0.8325	1.7091	24HR

(b) Four-day base estimator applied to independent sample

20-40N	28	-42.5392	4.7845	0.7353	2.5087	12HR
	57	-41.5999	5.1632	0.6698	2.9936	24HR
35-55N	33	-51.8999	4.5744	0.6777	2.6384	12HR
	50	-50.9419	5.0892	0.6999	2.8168	24HR
50-70N	26	-55.2345	4.4246	0.7689	2.1710	12HR
	47	-55.8510	4.2792	0.6703	2.4844	24HR

TABLE 12. Summary of NESC and FNWC independent regression test results. [Values are fractional explained variance (R^2).]

	NESC 500 mb				FNWC 500 mb			
	Band 1	Band 2	Band 3	Band Avg.	Band 1	Band 2	Band 3	Band Avg.
Three-day	0.7746	0.8055	0.9305	0.8369	0.7943	0.7591	0.7640	0.7725
Four-day	0.7892	0.8434	0.8922	0.8416	0.7984	0.7598	0.8031	0.7871
Period Avg.	0.7819	0.8244	0.9114	0.8392	0.7964	0.7594	0.7836	0.7798
	NESC 300 mb				FNWC 300 mb			
	Band 1	Band 2	Band 3	Band Avg.	Band 1	Band 2	Band 3	Band Avg.
Three-day	0.7575	0.7264	0.8684	0.7841	0.7468	0.6605	0.8439	0.7504
Four-day	0.6978	0.7053	0.7648	0.7226	0.6847	0.6915	0.6933	0.6898
Period Avg.	0.7276	0.7158	0.8166	0.7533	0.7158	0.6760	0.7686	0.7201
Avg. 500+300	0.7548	0.7701	0.8640	0.7962	0.7561	0.7177	0.7761	0.7499

VI. COMPARISONS OF INDEPENDENT TO DEPENDENT RESULTS

A summary of independent to dependent test results is given in Table 13. Three groups of tests are included. The first stratification (part a, Table 13) is averaged over all the bands and the data base modes. The outstanding aspect of part (a), column 2, is that it summarizes the comparative explained variances of T_F and T_N. The high explained variances for the dependent case at 500 mb may be noted, as well as the relatively modest decreases in R^2 (between 6 and 8%) upon testing with the independent pooled samples.

Part (b) of Table 13 averages over pressure levels and illustrates in summary form the distinction between the NESC and FNWC regression samples. These samples show the geographic patterns of R^2 noted earlier: e.g. R^2_N(dep) has a tendency to increase poleward whereas R^2_F(dep) has a band 2 minimum. The independent test column of part (b) summarizes the pattern of T_F-verification by bands (but independent of levels). Upon verification, the mean-regression R^2 shrinkage of T_F averages between 4 and 6% when all bands are considered.

Part (c) of Table 13 summarizes some of the key ideas put forth in earlier sections. For example, the variable T_N(5 dep) is characterized by a high value of R^2_N(5). The latter statistic decreases slightly (by about 5%) when

applied to independent-test data. The same remarks may be applied to $T_F(5)$ with slightly smaller $R_F^2(5) \simeq 0.874$ noted in the dependent case coupled with a somewhat larger shrinkage (about 9%) after test upon independent data. The conclusions regarding the comparative instability of the dependent test for $T_N(3)$ become clear from Table 13, part (c), where it is seen that the values of R^2 increase approximately 3% from dependent to independent tests.

The results for $T_F(3 \text{ dep})$ and $T_F(3 \text{ indep})$ are inconclusive in the form presented in Table 13(c). The whole set of results of part (c) indicates that little if any additional specification accuracy is obtained from the four-day data base in lieu of the three-day data base.

TABLE 13. Summary of independent to dependent test results.

	test being compared	dependent value of R^2	independent value of R^2
(a)	$T_N(5)$	0.8957	0.8392
	$T_F(5)$	0.8737	0.7798
	$T_N(3)$	0.7298	0.7533
	$T_F(3)$	0.7257	0.7201
(b)	T_N, band 1	0.7795	0.7548
	T_F, band 1	0.8248	0.7561
	T_N, band 2	0.7966	0.7701
	T_F, band 2	0.7532	0.7177
	T_N, band 3	0.8620	0.8640
	T_F, band 3	0.8212	0.7761
(c)	$T_N(5)$, 3 day	0.8989	0.8369
	$T_N(5)$, 4 day	0.8928	0.8369
	$T_N(3)$, 3 day	0.7465	0.7841
	$T_N(3)$, 4 day	0.7129	0.7226
	$T_F(5)$, 3 day	0.8760	0.7725
	$T_F(5)$, 4 day	0.8714	0.7871
	$T_F(3)$, 3 day	0.7247	0.7504
	$T_F(3)$, 4 day	0.7266	0.6898

VII. CONCLUSIONS

The results of Sections IV, V, and VI afford confirming evidence. For each case, high specification for T_N occurs at the 500-mb level. In spite of considerable shrinkage, there still remains a significant specification value of R^2 at 300 mb. This was true also of the FNWC specifications.

The reduction in R^2 associated with 300 mb T_N and T_F specifications was maximal in band 2 where more inter-diurnal variability in the temperature and associated tropopause conditions occur. The NESC specifications obtained by Smith et al (1970) by the 16-predictor equation also fell off to a relative minimum at the tropopause level in their SIRS-A test.

Not only is part of the observed lack of specification associated with the sampling of temperature extremes at or near the 300-mb level, but also the inter-diurnal variability in cloud cover would affect the noise contained in the radiances due to the cloud-correction technique, which is not error-free. The errors due to cloud-correction must be maximal in channels 2 and 3 for which maximum $d\tau/d\ln p$ weights occur in the upper troposphere. Hence, the mid-latitude band (band 2) which had most inter-diurnal as well as geographical sampling variability had the poorest 300-mb specification. On the other hand, the 500-mb specification and verification was adequate throughout. The

fact that the best 300-mb specification occurred in band 3 (50-70N) where cloud tops are climatologically lower than in the other two bands tends to confirm this conclusion. Similar tests at additional levels would have provided a better perspective in assessing the use of the SIRS corrected radiance data in constructing vertical profiles. As a result, a more balanced view of the vertical resolution afforded by the SIRS regression techniques would have evolved.

Several factors could work to improve the operational routine tested here: (1) to make use of a multi-level cloud-correction model for correction of SIRS-radiances (similar to that described by Smith et al 1970); (2) to employ a 16-predictor equation involving squares of radiances as well as linear terms; (3) to use a larger sample base confined to a smaller band zone, for example, 15^{o} latitude overlapping bands rather than the 20^{o} bands used here.

It is felt that with these modifications, a SIRS operational unit attached to FNWC could profitably use the SIRS data in improving their update analysis over sparse data regions, and in determining the onset of significant circulation changes.

LIST OF REFERENCES

1. Crow, E. L., Davis, F. A., Maxfield, M. W., Statistics Manual, U. S. Naval Ordnance Test Station, China Lake, California, 288 pp., 1955.

2. Dixon, W. J., Biomedical Computer Programs, Los Angeles Health Sciences Computing Facility, University of California, Los Angeles, 585 pp., 1966.

3. Haltiner, G. J., Numerical Weather Prediction, New York, John Wiley and Sons, 317 pp.,1971.

4. Smith, W. L., "Iterative Solution of the Radiative Transfer Equation for the Temperature and Absorbing Gas Profile of an Atmosphere," Applied Optics, Vol. 9, pp. 1993-1999, September 1970.

5. Smith, W. L., Woolf, H. M., and Jacob, W. J., "A Regression Method for Obtaining Real-Time Temperature and Geopotential Height Profiles from Satellite Spectrometer Measurements and its Application to NIMBUS III "SIRS" Observations," Monthly Weather Review, Vol. 98, pp. 582-603, August 1970.

INITIAL DISTRIBUTION LIST

		No. Copies
1.	Defense Documentation Center Cameron Station Alexandria, Virginia 22314	2
2.	Library, Code 0212 Naval Postgraduate School Monterey, California 93940	2
3.	Professor Frank L. Martin, Code 51Mr Department of Meteorology Naval Postgraduate School Monterey, California 93940	6
4.	Lieutenant Bruce W. Hepner U. S. NAVFAC GRAND TURK c/o NPO 558 Patrick AFB, Florida 32925	2
5.	Department of Meteorology, Code 51 Naval Postgraduate School Monterey, California 93940	3
6.	Naval Weather Service Command Naval Weather Service Headquarters Washington Navy Yard Washington, D. C. 20390	1

Security Classification

DOCUMENT CONTROL DATA - R & D

Security classification of title, body of abstract and indexing annotation must be entered when the overall report is classified)

1. ORIGINATING ACTIVITY *(Corporate author)*

Naval Postgraduate School
Monterey, California 93940

2a. REPORT SECURITY CLASSIFICATION

Unclassified

2b. GROUP

3. REPORT TITLE

Regression Relationships Between Satellite Infrared Radiance and Tropospheric Temperature

4. DESCRIPTIVE NOTES *(Type of report and, inclusive dates)*

Master's Thesis; March 1972

5. AUTHOR(S) *(First name, middle initial, last name)*

Bruce W. Hepner

6. REPORT DATE	7a. TOTAL NO. OF PAGES	7b. NO. OF REFS
March 1972	50	5

8a. CONTRACT OR GRANT NO.	9a. ORIGINATOR'S REPORT NUMBER(S)
b. PROJECT NO.	
c.	9b. OTHER REPORT NO(S) *(Any other numbers that may be assigned this report)*
d.	

10. DISTRIBUTION STATEMENT

Approved for public release; distribution unlimited.

11. SUPPLEMENTARY NOTES	12. SPONSORING MILITARY ACTIVITY
	Naval Postgraduate School Monterey, California 93940

13. ABSTRACT

Global temperatures are obtained using a linear least squares regression method with satellite radiation measurements, particularly those obtained from the SIRS-B aboard the NIMBUS IV satellite. Regression equations relating temperature to spectral radiance observations are employed. The regression equations were then applied to independent observations to determine the feasibility of temperature determinations over sparse data regions.

DD FORM 1 NOV 65 1473 (PAGE 1)

S/N 0101-807-6811

Security Classification

A-31408

KEY WORDS	LINK A		LINK B		LINK C	
	ROLE	WT	ROLE	WT	ROLE	WT
eight predictor						
regression equations						
SIRS-B radiances						

Thesis
H486
c.1

133940

Hepner

Regression relationships between satellite infrared radiance and tropospheric temperature.